On stability of a clamped-pinned pipe conveying fluid

G.L. Kuiper and A.V. Metrikine

Faculty of Civil Engineering and Geosciences, Delft University of Technology, Delft, The Netherlands

In the past, stability of an undamped clamped-pinned pipe conveying fluid has been always considered numerically leading to controversial results. Païdoussis (2004) has shown that a numerical stability analysis of a clamped-pinned pipe requires exceptionally large number of vibration modes to obtain the correct dynamical behaviour. In this paper, analytical proof of stability of a clamped-pinned pipe conveying fluid at a low speed is given. A tensioned Euler-Bernoulli beam in combination with a plug flow model is used as a model. The stability is studied employing a D-decomposition method. Advantages and disadvantages of this method with respect to the conventional methods are discussed. For demonstration of the method's capabilities, it is applied to a clamped-pinned pipe subject to linearised Morison damping caused by the surrounding fluid.

Key words: pipe conveying fluid, stability, D-decomposition method

1 Introduction

In the offshore industry vertical pipes are used to carry oil from a well under the sea bottom to a floating facility. The part of the pipe from the sea bottom to the floating platform is called the riser and is shown in Figure 1. The internal fluid speed of the oil is small (less than 1 m/s) and normally disregarded in the riser analysis. However, some numerical analyses (Païdoussis, 2004) showed large riser deflections due to such small fluid speed. As the author explained, this was purely caused by numerical errors.

The dynamics and stability of pipes conveying fluid has been studied thoroughly in the last decades. Comprehensive reviews on these issues are given in two books of Païdoussis (1998, 2004). For pipes of a finite length, the dynamical behaviour depends strongly on the type of boundary conditions at both ends (Lee and Mote, 1997). Distinction should be made between the type of supports (fixed, simple, free, inertial, etc.) and their location (upstream or downstream). In this paper we refer to a fixed and simple supports as to *clamped* and *pinned*, respectively. Besides, referring to a *clamped-pinned* pipe we mean that the clamped end is located upstream.

It is known that a tensioned pipe conveying fluid and having symmetrical boundary conditions (*clamped-clamped, pinned-pinned*, etc.) behaves as a conservative gyroscopic system (Païdoussis, 1998), implying that the total energy of the system varies periodically in time. For small fluid velocities such pipes are stable. After a certain critical flow velocity they lose stability, i.e. if the model is linear, the pipe displacements grow exponentially in time. Flow velocities lower and higher than the critical velocity are denoted in this paper as sub-critical and super-critical, respectively.

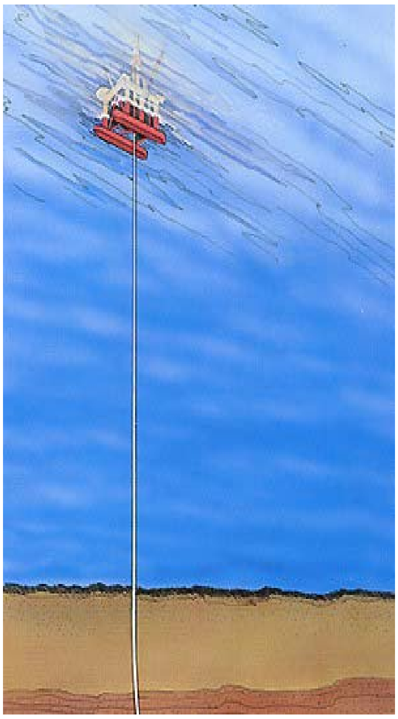

Figure 1: A riser conveying oil from the well to the floating platform.

The dynamics of systems with mixed support conditions is more complicated and resulted even in a theoretically predicted contradiction. Païdoussis (2004) studied numerically pinned-clamped and clamped-pinned pipes conveying fluid. He found that to predict the dynamical behaviour of the clamped-pinned pipe, even 8 significant-figure accuracy was not good enough. The imaginary part of the complex eigen frequency seemed to be negative, implying unstable behaviour for any flow velocity greater than zero. On the other hand, Lee and Mote (1997) who analysed the energetics of flexible pipes conveying fluid found no energy grow for the clamped-pinned boundary conditions. Similar contradictions were observed for shells conveying fluid (Zolotarev, 1987; Misra et al., 2001). The main goal of this paper is to prove *analytically* that a clamped-pinned pipe conveying fluid at a low speed is stable. The proof is carried out employing a D-decomposition method, demonstration of its capabilities is the second main goal of the paper. The D-decomposition method was developed for stability analyses of linear dynamical systems (Neimark 1978; Neimark et al. 2003). Since then, this method has been successfully applied in the control theory, in electric, mechanical and civil engineering. Recently, this method has shown to be very useful for stability analysis of high-speed trains (Denisov et al., 1985; Metrikine and Popp, 1999; Metrikine and Verichev, 2001; Zheng et al., 2000). According to the knowledge of the authors, the D-decomposition method, however, has never been used for determining stability of pipes conveying fluid. Therefore, advantages and disadvantages of this method in comparison with the conventional ones are discussed in this paper. The paper is structured as follows. Section 2 presents a mathematical statement of the problem, which describes small vibrations of a finite-length pipe conveying fluid. The forces due to the external surrounding water are modelled with the help of the linearised Morison formula. Having obtained the characteristic equation for the pipe in Section 2, conventional methods of analysis of the roots of this equation are discussed in Section 3 and briefly compared to the D-decomposition method. Section 4 is devoted to a short description of the D-decomposition method in application to the pipe stability. Section 5 presents an analytical proof of the stability of an undamped clamped-pinned pipe by disregarding the drag. This can be considered as a pipe conveying fluid surrounded by air. In Section 6, capabilities of the D-decomposition method are demonstrated accounting for the drag described by the Morison equation.

2 Statement of the problem and characteristic equation

The system under consideration is an initially straight, tensioned, fluid-conveying pipe of a finite length. In reality, the axial tension in the riser is a linear function of depth caused by its submerged dead weight. For simplicity, a pipe is analysed with a constant tension equal to the effective top tension for a riser with the same dimensions. Due to this simplification the riser behaves somewhat stiffer. The pipe conveying fluid is sketched in Figure 2 and is plotted horizontally to visualize the constant tension. It is assumed that the riser moves only in the plane that is depicted in the figure. The pipe is considered to be slender, and its lateral motion $w(x,t)$, to be small and of a long wavelength as compared to the diameter of the pipe so that the Euler-Bernoulli theory is applicable for description of the pipe dynamic bending. The equation of motion governing the lateral in-plane motion of the pipe without internal and external fluid as a function of the axial distance *x* and time *t* reads

$$EI\frac{\partial^4 w}{\partial x^4} - T\frac{\partial^2 w}{\partial x^2} + m_r\frac{\partial^2 w}{\partial t^2} = f_{\text{int}}(x,t) + f_{ext}(x,t) \; , \tag{1}$$

where *EI* is the bending stiffness of the pipe, m_r is the mass of the pipe per unit length, *T* is a prescribed axial tension, $f_{\text{int}}(x,t)$ and $f_{ext}(x,t)$ are forces acting on the pipe from inside and outside, respectively.

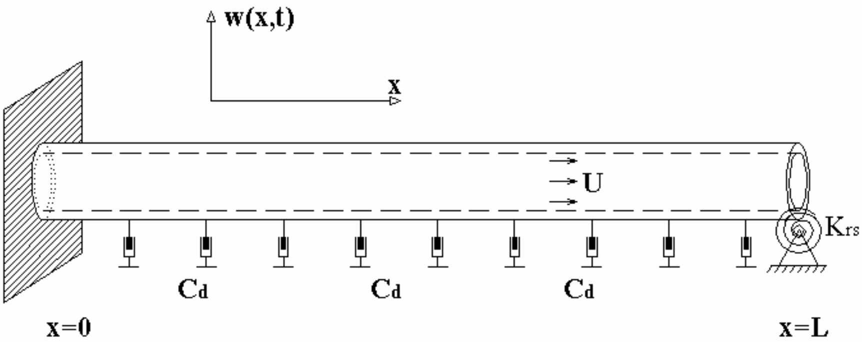

Figure 2: A pipe conveying fluid.

The internal fluid flow is approximated as a plug flow, i.e. as if it were an infinitely flexible rod travelling through the pipe, all points of the fluid having a velocity U relative to the pipe. This is a reasonable approximation for a fully developed turbulent flow profile (Païdoussis, 1998). The inertia force exerted by the internal plug flow on the pipe, can be written as

$$f_{\text{int}} = -m_f \left.\frac{d^2w}{dt^2}\right|_{x=Ut}, \tag{2}$$

where m_f is the fluid mass per unit length, U is the flow velocity. The total acceleration of the fluid mass can be decomposed into a local, Coriolis and centrifugal acceleration:

$$\begin{aligned} m_f \left.\frac{d^2w}{dt^2}\right|_{x=Ut} &= m_f \left\{ \frac{d}{dt}\left(\frac{\partial w}{\partial t} + \frac{\partial w}{\partial x}\frac{dx}{dt} \right)\bigg|_{x=Ut} \right\} = m_f \left\{ \frac{d}{dt}\left(\frac{\partial w}{\partial t} + U\frac{\partial w}{\partial x} \right)\bigg|_{x=Ut} \right\} \\ &= m_f \left\{ \frac{\partial^2 w}{\partial t^2} + 2U\frac{\partial^2 w}{\partial x \partial t} + U^2 \frac{\partial^2 w}{\partial x^2} \right\} \end{aligned} \tag{3}$$

The general practice in the offshore industry for modelling the hydrodynamic force due to the surrounding water is based on the Morison formula. This formula presents the hydrodynamic force as a superposition of an inertia force and a drag force. The inertia force is proportional to the acceleration of the pipe. The drag force depends on the velocity of the pipe non-linearly. In what follows, this non-linearity is neglected and the following linearised expression is assumed to be representative for a pipe in a non-moving fluid (Païdoussis, 1998)

$$f_{ext}(x,t) = -\rho_f A_e C_a \frac{\partial^2 w}{\partial t^2} - \frac{1}{2}\rho_f D\tilde{C}_d \frac{\partial w}{\partial t} \ , \tag{4}$$

where ρ_f is the density of the surrounding fluid, A_e is the external cross section of the pipe, C_a is the added mass coefficient, D is the external diameter of the pipe, C_d is the adapted, linearised drag coefficient with the dimension of velocity.

The external and internal fluid cause a hydrostatic pressure on the pipe wall. This can easily be incorporated by changing the true axial tension into a so-called effective tension

$$T_{eff} = T + A_e p_e - A_i p_i \ , \tag{5}$$

where A_e and A_i are the external and internal cross sectional areas of the pipe, and, p_e and p_i are the hydrostatic pressures outside and inside the pipe. Combining Eqs (1)-(5) the resulting equation of motion for a pipe conveying fluid can be written as

$$EI\frac{\partial^4 w}{\partial x^4} + \left(m_f U^2 - T_{eff}\right)\frac{\partial^2 w}{\partial x^2} + 2m_f U\frac{\partial^2 w}{\partial x \partial t} + m\frac{\partial^2 w}{\partial t^2} + \frac{1}{2}\rho_f D C_d \frac{\partial w}{\partial t} = 0 \ , \tag{6}$$

in which

$$m = m_r + m_f + \rho_f A_e C_a$$

The upstream end of the pipe is rigidly connected to the sea bottom, whereas the downstream end is flexibly connected to the floating platform. This connection is assumed to allow no lateral displacement but to provide a restoring moment proportional to the rotation angle of the pipe. The clamped-pinned pipe is obtained from this formulation in the limit of the restoring rotational moment going to zero. Thus, the boundary conditions at the ends of the pipe are given as

$$w(0,t) = 0 \tag{7}$$

$$\frac{\partial w(0,t)}{\partial t} = 0 \tag{8}$$

$$EI\frac{\partial^2 w(L,t)}{\partial x^2} = -K_{rs}\frac{\partial w(L,t)}{\partial x} \tag{9}$$

$$w(L,t) = 0 \tag{10}$$

where K_{rs} is the stiffness of the rotational spring at the downstream end. Introducing the following dimensionless variables and parameters

$$\eta = w/L\ ,\ \xi = x/L\ ,\ \tau = t\sqrt{EI/m}\Big/L^2\ ,\ V = U\sqrt{m_f/T_{eff}}\ ,\ \kappa = K_{rs}L/EI\ ,$$
$$\alpha = L\sqrt{\left(T_{eff}m_f\right)\big/\left(mEI\right)}\ ,\ \beta = L^2\,T_{eff}/EI\ ,\ \gamma = \rho_f DC_d L^2\Big/\left(2\sqrt{mEI}\right)\ ,$$

the statement of the problem Eqs. (6)-(10) is rewritten as

$$\frac{\partial^4\eta}{\partial\xi^4}+\beta\left(V^2-1\right)\frac{\partial^2\eta}{\partial\xi^2}+2\alpha V\frac{\partial^2\eta}{\partial\xi\partial\tau}+\frac{\partial^2\eta}{\partial\tau^2}+\gamma\frac{\partial\eta}{\partial\tau}=0\ , \tag{11}$$

$$\eta(0,\tau)=0\ ,\quad \frac{\partial\eta(0,\tau)}{\partial\xi}=0\ ,\quad \frac{\partial^2\eta(1,\tau)}{\partial\xi^2}=-\kappa\frac{\partial\eta(1,\tau)}{\partial\xi}\ ,\quad \eta(1,\tau)=0\ . \tag{12}$$

To find the eigenvalues of the problem (11)-(12), which determine the stability of the pipe, the displacement $\eta(\xi,\tau)$ is to be sought in the following form

$$\eta(\xi,\tau)=W(\xi)e^{\lambda\tau}\ . \tag{13}$$

The pipe is unstable if at least one of the eigenvalues λ has a positive real part. Substituting Eq.(13) into the equation of motion (11), the following ordinary differential equation is obtained

$$\frac{d^4W}{d\xi^4}+\beta\left(V^2-1\right)\frac{d^2W}{d\xi^2}+2\alpha V\lambda\frac{dW}{d\xi}+\lambda^2W+\gamma\lambda W=0 \tag{14}$$

The general solution to this equation is given by

$$W(\xi)=\sum_{j=1}^{4}C_je^{ik_j\xi}\ , \tag{15}$$

where C_j are amplitudes of vibrations and k_j are the wavenumbers. Substituting solution Eq.(15) into Eq.(14), a relationship is obtained between the wavenumbers k_j and the eigenvalues λ:

$$k_j^{\,4}-\beta\left(V^2-1\right)k_j^{\,2}+2\alpha V\lambda ik_j+\lambda^2+\gamma\lambda=0\ . \tag{16}$$

From this relationship four wavenumbers k_j can be determined as functions of λ and the pipe parameters. To find the four unknown amplitudes $C_j, j=1..4$, Eq.(15) should be substituted into the boundary conditions Eq.(12). This yields the following system of four linear algebraic equations:

$$\sum_{j=1}^{4} C_j = 0\,,\quad \sum_{j=1}^{4} ik_j C_j = 0\,,\quad \sum_{j=1}^{4}\left(\left(-k_j + i\kappa\right)k_j e^{ik_j} C_j\right) = 0\,,\quad \sum_{j=1}^{4} e^{ik_j} C_j = 0\,. \tag{17}$$

This system of equations has a non-trivial solution if, and only if its determinant Δ is equal to zero, which leads to the characteristic equation Δ=0. The determinant Δ can be calculated analytically to give expression Eq.(A1), which is given in Appendix A.

Now that the characteristic equation has been obtained, its roots λ have to be analysed to draw a conclusion on the pipe stability. In this paper, a so-called D-decomposition method (Neimark 1978; Neimark et al. 2003) is used to this end. Before that, however, conventional methods of analysis of the characteristic equation are discussed in short and the reasons are formulated for application of the D-decomposition method.

3 Methods of analysis of the characteristic equation

In general, the roots of the characteristic equation for a pipe conveying fluid cannot be expressed explicitly. Consequently, there exist several numerical approaches to determine these roots, see (Païdoussis, 1998). Here only the two most used methods are mentioned. The first one is a straightforward numerical solution of the characteristic equation. The main shortcoming of this method is that a special study is necessary to prove that all roots in a chosen complex domain have been found. The second approach makes use of the Galerkin method and the Argand diagram. The reason to apply the Galerkin method is that a pipe conveying fluid does not possess normal modes with fixed nodal points. The Argand diagram is used to plot the position of the eigenvalues in the complex λ-plane using the flow speed as the parameter. It is not always straightforward to find an optimal modal basis for approximating the solution, like in the case that a boundary is connected to inertial, elastic or viscous elements.

The D-decomposition method, which is used in this paper, is, in our view, a very convenient method for stability analysis of linear systems. The main advantage of this method relative to the abovementioned ones is that it does not require searching for complex zeroes of a complex function. The stability can be analysed using the D-decomposition method by just considering the imaginary axis of the complex λ-plane (the plane of complex eigenvalues). This increases the accuracy of the stability prediction and, in some cases, the calculation speed.

In this paper, the D-decomposition method is first used for an analytical proof that an undamped clamped-pinned pipe conveying fluid at a low speed is stable. Then, advantages of this method are demonstrated considering the pipe surrounded by water.

4 D-decomposition method in application to pipes conveying fluid

Since the D-decomposition method is not a conventional tool in studies on stability of pipes, it is worth to explain the idea of the method and the manner in which it can be applied to a finite-length pipe conveying fluid. The D-decomposition method utilises the fact that the stability of a linear system is fully determined by the sign of the real part of its eigenvalues λ. Eigenvalues which are located in the right half-plane of the complex λ-plane correspond to unstable vibrations, see Figure 3. Consequently, the imaginary axis of this plane, $\lambda = i\Omega, \Omega \in \Re$ is the boundary that separates the "stable" and "unstable" eigenvalues (roots with $\mathrm{Re}(\lambda) < 0$ and $\mathrm{Re}(\lambda) > 0$, respectively). Assume now that the characteristic equation contains a parameter *P* that can be expressed explicitly as a function of all the other system parameters. Such expression can then be used as a rule to map the imaginary axis of the λ-plane onto the complex plane of the parameter *P* as sketched in Figure 3. The frequency *Ω* serves as the parameter of this mapping. The resulting mapped line(s), which are referred to as D-decomposition line(s), breaks the *P*-plane into domains with different number of "unstable" eigenvalues. Within a domain, this number does not vary.

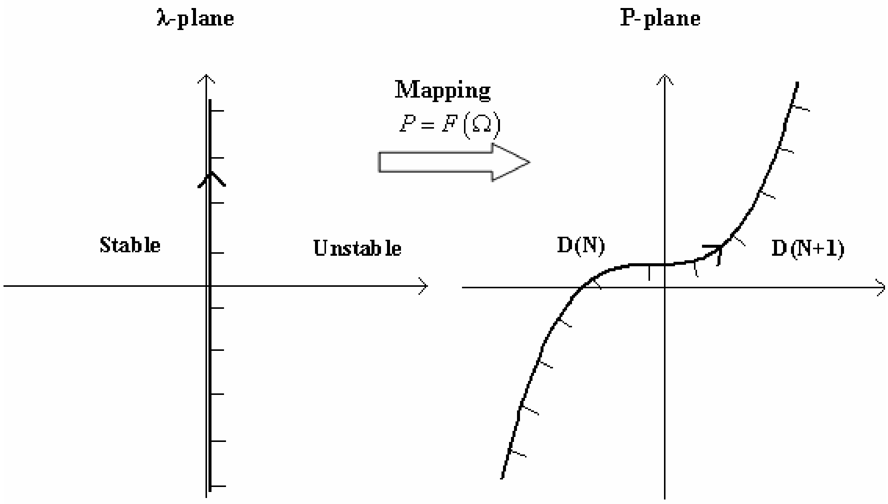

Figure 3: A graphical representation of the D-decomposition method. The notation $D(N)$ implies that there are N "unstable" eigenvalues in the domain.

Shading the right side of the imaginary axis of the λ-plane (the side of "unstable" eigenvalues), and keeping the shading at the corresponding side of the D-decomposition line(s), the information containing in the decomposed P-plane can be enriched. With this shading, it becomes known that passing through a D-decomposition line in the direction of shading corresponds to the gain of one additional "unstable" eigenvalue by the characteristic equation. Thus, if the number of the "unstable" eigenvalues is known for only one (arbitrary) value of the parameter P, the D-decomposed P-plane allows to draw a conclusion on stability of the system for all admissible values of this parameter at once.

As compared to the conventional methods of analysis, the D-decomposition method has both advantages and disadvantages. The main advantage becomes apparent if a parametric study of stability should be performed. A D-decomposed plane of a parameter P contains information on stability of the system for all values of P, whereas the Argand diagram, for example, indicates the stability for a specific value of this parameter, only (if this parameter is not the fluid speed). Another advantage of the D-decomposition method is that it is equally applicable to pipes with any (linear) boundary conditions. For applying this method, no introduction of comparison functions is necessary (which takes quite an experience), like in the case of Galerkin method.

The major disadvantage of the D-decomposition method is that having decomposed the plane of a parameter, it is still necessary to know the number of "unstable" eigenvalues for a specific, though arbitrary, value of this parameter. To find this number is not necessarily an easy task, although it can always be done by using *the principle of the argument* (see Fuchs *et* al., 1964, and, in combination with the D-decomposition method, Verichev and Metrikine, 2002). The other possibilities are to combine the D-decomposition method with the classical one or (the best, if possible) to use a degenerate value of the parameter, for which the system stability is known either from physical considerations or previous research. The latter approach is applied in this paper.

As follows from the above-given short description of the D-decomposition method, to apply this method efficiently, the characteristic equation should contain a parameter that can be expressed explicitly. Characteristic equations of pipes conveying fluid do not necessarily contain such a parameter. By changing a boundary condition (extra mass, stiffness, dashpot, etc.), the boundary element enters the characteristic equation in such a way that it can be expressed explicitly as a function of all the other system parameters. For the clamped-pinned pipe the rotational spring is introduced for this purpose at the right end of the pipe, see Figure 2 and Eq.(9). If the stiffness of this spring is zero, then the clamped-pinned pipe is retrieved. On the other hand, if this stiffness tends to infinity, the right end of the pipe becomes fixed.

As can be seen from Eq.(A1) (Appendix A), the characteristic equation for the pipe at hand consists of two parts, one proportional to the dimensionless rotational stiffness κ and the other part independent of this stiffness:

$$\Delta = \kappa A(\Omega) + B(\Omega) = 0 \tag{18}$$

where A and B are functions of Ω obtained by using the relationship between the wavenumbers k_j and the eigenvalues λ (Eq.(16)) and the expression $\lambda = i\Omega$. Expressing the rotational stiffness from Eq.(18), the rule is obtained for mapping the imaginary axis of the λ-plane onto the plane of the parameter κ:

$$\kappa = -\frac{B(\Omega)}{A(\Omega)} \tag{19}$$

Note that in the complex κ-plane the positive part of the real axis only has physical meaning, since κ is the stiffness of the rotational spring.

In the next section, the mapping rule (19) is used for an analytical study of stability of the clamped-pinned pipe conveying fluid at a low speed, i.e. far below the critical velocity. In section 6, this rule is applied to the pipe subject to linearised Morison damping as described by Eq.(4).

5 Undamped clamped-pinned pipe

In this section, the D-decomposition method is applied to prove analytically that a clamped-pinned pipe conveying fluid and subject to no damping is stable at low fluid speeds, since numerical solutions could not prove this. Setting the adapted, linearised damping coefficient C_d to zero, the relationship between the wavenumbers k_j and the eigenvalues λ, Eq.(16), reduces to

$$k_j^{\,4} - \beta\left(V^2 - 1\right)k_j^{\,2} + 2\alpha V \lambda i k_j + \lambda^2 = 0 \tag{20}$$

To apply the D-decomposition method, the imaginary axis of the λ-plane has to be mapped. To this end, λ should be considered in the form $\lambda = i\Omega$, with Ω a real value, which has to be varied from minus infinity to plus infinity. Substitution of this relationship into Eq.(20) yields the following dispersion equation:

$$k_j^{\,4} - \beta\left(V^2 - 1\right)k_j^{\,2} - 2\alpha V \Omega k_j - \Omega^2 = 0 \tag{21}$$

The physical meaning of Eq.(21) is that it determines the wavenumbers of waves, which would be generated in a pipe by a harmonic load of frequency Ω .

To accomplish the mapping defined by Eq.(19), complex values *A* and *B* should be known as functions of the angular frequency Ω. In principle, *A* and *B* could be calculated numerically by using a program for finding complex roots of a polynomial. However, in the particular case at hand, direct numerical calculation is not suitable, since it would give a big error when calculating the imaginary part of the ratio B/A. The origin of this error is that this ratio is purely real, as it is shown analytically below.

To analyse *A* and *B*, wavenumbers k_j should first be studied as functions of the frequency Ω. This is done with the help of the Descartes-Euler Solution in combination with the Cardan's Solution (Korn and Korn, 1961). The dispersion equation Eq.(21) is a quartic equation with respect to the wavenumbers k_j, which can be rewritten as

$$k_j^{\ 4} + p_4 k_j^{\ 2} + q_4 k_j + r_4 = 0 \tag{22}$$

with

$$p_4 = -\beta\left(V^2 - 1\right),\ \ q_4 = -2\alpha V\Omega,\ \ r_4 = -\Omega^2 \tag{23}$$

In accordance with the Descartes-Euler solution (Korn and Korn 1961), the roots of this equation are the four sums (+++, +--, -+-, --+)

$$\pm\sqrt{z_1} \pm \sqrt{z_2} \pm \sqrt{z_3} \tag{24}$$

with the signs of the square roots chosen so that

$$\sqrt{z_1}\sqrt{z_2}\sqrt{z_3} = -q_4/8 = V\alpha\Omega / 4 \tag{25}$$

where z_1, z_2 and z_3 are the roots of the cubic equation

$$z^3 + \frac{p_4}{2} z^2 + \frac{p_4^{\ 2} - 4r_4}{16} z - \frac{q_4^{\ 2}}{64} = 0 \tag{26}$$

The cubic equation Eq.(26) can be solved by using the Cardan's Solution (Korn and Korn, 1961). In accordance with this solution, Eq.(26) should first be transformed to the so-called "reduced" form through the substitution $z = y - p_4/6$. This yields

$$y^3 + p_3 y + q_3 = 0 \tag{27}$$

with

$$p_3 = -\frac{1}{3}\left(\frac{p_4}{2}\right)^2 + \frac{{p_4}^2 - 4r_4}{16} = -\frac{\beta^2\left(V^2-1\right)^2}{48} + \frac{\Omega^2}{4}$$

$$q_3 = \frac{2}{27}\left(\frac{p_4}{2}\right)^3 - \frac{1}{3}\frac{p_4}{2}\frac{{p_4}^2 - 4r_4}{16} - \frac{{q_4}^2}{64} = \frac{\beta^3\left(V^2-1\right)^3}{864} + \frac{\Omega^2\beta\left(V^2-1\right)}{24} - \frac{(V\alpha\Omega)^2}{16} \ ,$$

The roots of the "reduced" cubic equation Eq.(27) are

$$y_1 = X + Y \ , \quad y_{2,3} = -\frac{X+Y}{2} \pm i\frac{X-Y}{2}\sqrt{3} \ ,$$

with

$$X = \sqrt[3]{-\frac{q_3}{2} + \sqrt{Q}} \ , \qquad Y = \sqrt[3]{-\frac{q_3}{2} - \sqrt{Q}} \ ,$$

$$Q = \left(\frac{p_3}{3}\right)^3 + \left(\frac{q_3}{2}\right)^2 = \left[\frac{1}{1728}\right]\Omega^6 + \left[-\frac{\beta^2\left(V^2-1\right)^2}{6912} + \left(\frac{\beta\left(V^2-1\right)}{48} - \frac{V^2\alpha^2}{32}\right)^2\right]\Omega^4$$

$$+\left[\frac{\beta^4\left(V^2-1\right)^4}{27648} - \frac{\beta^3\left(V^2-1\right)^3 V^2\alpha^2}{27648}\right]\Omega^2 \ . \tag{28}$$

Depending on the parameter Q, the cubic equation Eq.(27) has one real root and two conjugate complex roots, three real roots of which at least two are equal, or three different real roots, if Q is positive, zero, or negative, respectively. All the terms in square brackets in Eq.(28) are positive if the dimensionless fluid velocity V is smaller than unity (which is lower than the critical velocity). Consequently, for these fluid velocities, the value of Q is positive for all real frequencies Ω (except for zero frequency). Thus, the "reduced" cubic equation Eq.(27) has one real and two complex conjugate roots. The cubic equation Eq.(26) with respect to Z possesses the same type of roots (one real and two complex conjugate) since $z = y - p_4/6$ and p_4 is a real value. These roots can be written as

$$z_1 = a \ , \quad z_2 = b + ic \ , \quad z_3 = b - ic \tag{29}$$

with a, b and c real values.

Thus, the roots of the dispersion equation, Eq.(21), can be written as (the plus sign in front of a square root implies that the real part of this root is positive)

$$k_1 = \sqrt{a} \times \mathrm{signum}(\Omega) + \sqrt{b+ic} + \sqrt{b-ic}$$

$$k_2 = \sqrt{a} \times \mathrm{signum}(\Omega) - \sqrt{b+ic} - \sqrt{b-ic}$$

$$k_3 = -\sqrt{a} \times \mathrm{signum}(\Omega) - \sqrt{b+ic} + \sqrt{b-ic}$$

$$k_4 = -\sqrt{a} \times \mathrm{signum}(\Omega) + \sqrt{b+ic} - \sqrt{b-ic} \tag{30}$$

The four roots given by Eqs.(30) have been chosen from the eight combinations presented by Eq.(24) so that Eq.(25) is satisfied. Taking into account that a must be positive and real as can be shown by substitution of Eqs.(29) into Eq.(25), it is easy to conclude from Eq.(30) that k_1 and k_2 are real, whereas k_3 and k_4 are complex conjugate. Employing this information and using the fact that $k_1 + k_2 + k_3 + k_4 = 0$ (see Eqs.(30)), the following purely imaginary expressions are found for *A* and *B*:

$$\begin{aligned}
A = i\Big\{ & 4\left(k_2^2 + 2k_2k_3^R - 3\left(k_3^R\right)^2 - \left(k_3^R\right)^2\right)\sinh\left(Lk_3^I\right)\sin\left(L\left(k_2 + k_3^R\right)\right) \\
& +8k_3^I\cosh\left(Lk_3^I\right)\cos\left(L\left(k_2 + k_3^R\right)\right) - 8k_3^I\left(k_2 + k_3^R\right)\cos(2Lk_3^R)\Big\} \\
B = i\Big\{ & -4k_3^I\left(k_2^2 + 2k_2k_3^R + 5\left(k_3^R\right)^2 + \left(k_3^I\right)^2\right)\cosh\left(Lk_3^I\right)\sin\left(L\left(k_2 + k_3^R\right)\right) \\
& +4\left(k_2 + k_3^R\right)\left(k_2^2 + 2k_2k_3^R - 3\left(k_3^R\right)^2 + \left(k_3^I\right)^2\right)\sinh\left(Lk_3^I\right)\cos\left(L\left(k_2 + k_3^R\right)\right) \\
& +16k_3^Rk_3^I\left(k_2 + k_3^R\right)\sin(2Lk_3^R)\Big\}
\end{aligned} \tag{31}$$

Since in Eq.(31) only real variables are used, the ratio B/A is purely real as well. Having found *A* and *B*, it becomes easy to accomplish the mapping given by Eq.(19). However, because of the real ratio B/A, the mapped lines in the complex κ-plane are all located on the real axis (see Figure 4). These lines run up and down the real axis, tending to the plus and minus infinity for frequencies which turn *A* to zero. It is easy to understand that the frequencies turning the ratio B/A to infinity are the natural frequencies of the clamped-clamped pipe (since the characteristic equation for this pipe is $A = 0$ as can be obtained from Eq.(A1) in the limit $\kappa \to \infty$). The natural frequencies of the clamped–pinned pipe correspond to the zeroes of *B*. Thus, varying the frequency *Ω* while performing the mapping, the natural frequencies of the clamped-pinned pipe are found as the mapped line crosses the origin of the κ-plane. Since the mapped line crosses the origin infinitely many times, one may conclude that the clamped-pinned pipe has infinitely many real natural frequencies, as the speed of the fluid flow is low. This does not prove, however, that there are no complex natural frequencies of the pipe in this case.

To prove the absence of natural frequencies with a positive imaginary part (i.e., to prove the pipe's stability), we make use of a so-called principle of limiting absorption (Matania and Devinatz, 1987).

This principle is based on an obvious fact that all physical systems are damped by a dissipation mechanism. Thus, each physically relevant model without explicitly accounted damping must give the same results as those obtained from the same model but with damping included by tending the damping to zero in the final results. This principle is widely used in problems of radiation and diffraction of waves (Ginzburg, 1990; Ginzburg and Tsytovich, 1990).

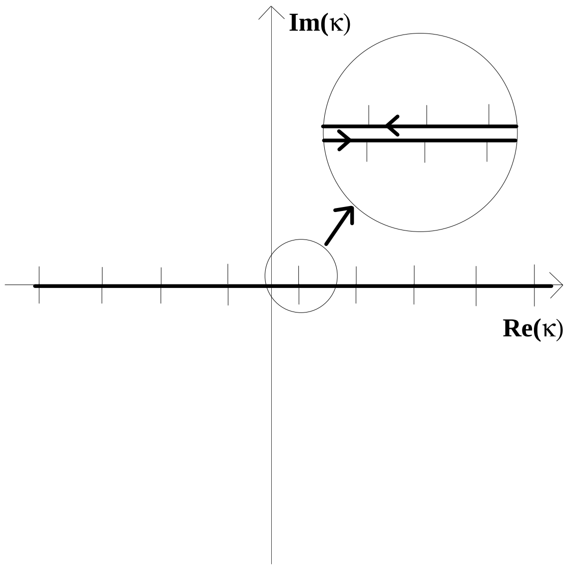

Figure 4: D-decomposition of the complex κ-plane for $V < 1$.

Thus, to be sure that the results of an undamped model are physically correct, we first should include the damping into the model, study it, and then carry out the limiting transition to zero damping. This approach however, is quite laborious and therefore researchers have found easier ways to comply with the principle (Ginzburg, 1990) without introducing damping. In application to the stability problems, the trick is not to consider the imaginary axis of the complex λ-plane as the boundary between the "stable" and "unstable" eigenvalues but a parallel line that lies a bit to the right from this axis. The background of this trick is very transparent. Indeed, introduction of a damping mechanism shifts the eigenvalues to the left in the complex λ-plane. One of the ways to account for this shift is to keep the eigenvalues at place (introducing no damping) but shift the imaginary axis of the λ-plane to the right.

Let us apply this way of analysis and map the line $\lambda = \sigma + i\Omega$; $\sigma, \Omega \in \Re; \sigma > 0$ onto the complex κ-plane by varying λ from minus infinity to plus infinity (using Eq.(19)). Considering the dimensionless parameter σ as small $\sigma << 1$ the D-decomposition of the κ-plane is obtained that is shown in Figure 5. Only the lines closest to the real axis are shown, which correspond to low values of the frequency Ω (increasing the frequency, a countable number of lines can be obtained). The number $D(N)$ of "unstable" eigenvalues in every domain of the decomposed plane corresponds to the pipe at hand, whose vibrational energy is slightly dissipated by a dissipation mechanism. The smaller the parameter σ, the smaller the dissipation.

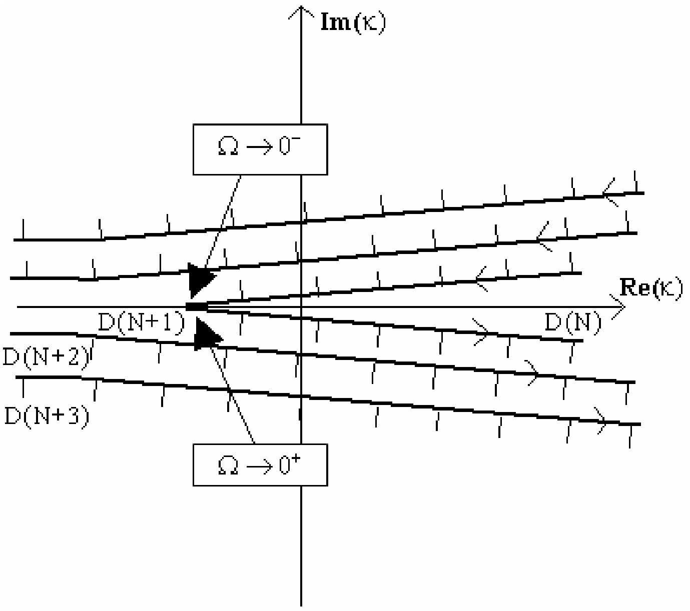

Figure 5: Result of the mapping of the line $\lambda = i\Omega + \sigma,\ \sigma << 1$ *onto the* κ*-plane for* $V < 1$.

Studying the effect of the parameter σ on the result of D-decomposition presented in Figure 5, it turned out that the smaller the parameter σ, the closer the D-decomposition lines to the real axis. In the limit $\sigma \to 0$ they all tend to the real axis, i.e. to the situation presented in Figure 4. This implies that there exists a uniform convergence of the results with respect to the parameter σ. Thus, conclusions, which are drawn from Figure 5 on the pipe's stability, are valid for the case without damping as well for the case with an infinitely small damping.

Figure 5 shows that the D-decomposition lines do not cross the positive part of the real axis. This implies that the number of "unstable" eigenvalues does not depend on the rotational stiffness of the pipe's support (the physically admissible values of this stiffness are real and positive). In particular, this implies that the number of unstable roots for the clamped-clamped pipe ($\kappa \to \infty$) is the same as for the clamped-pinned pipe ($\kappa = 0$). Thus, since it is well known (Païdoussis 1998) that the clamped-clamped pipe is stable at small fluid speeds, we can conclude that the clamped-pinned pipe is stable at these speeds as well.

Let us note that for this conclusion to be true, it is essential that the point $D_{\Omega=0}$ of the D-decomposition curves, which corresponds to zero frequency $\Omega = 0$ is located on the negative part of the real κ-axis, see Figure 5. In the opposite case, the clamped-pinned and clamped-clamped pipes would have a different number of unstable eigenvalues. To prove that the point $D_{\Omega=0}$ always lies on the negative semi-axis, analytical evaluations can be performed that are shown below. Using program MAPLE, it is possible to calculate the limit of A and B in Eq.(19) as the frequency Ω goes to zero. This limit is given as

$$D_{\Omega=0} = \lim_{\Omega \to 0} \kappa = -\frac{\psi^2 + e^{2\psi}\psi^2 - e^{2\psi}\psi + \psi}{e^{2\psi}\psi + 4e^{\psi} - 2 - 2e^{2\psi} - \psi}, \; \psi = \sqrt{\beta\left(1 - V^2\right)}, \tag{32}$$

It is easy to show that $\lim_{\Omega \to 0} \kappa$ is real and positive as long as ψ is real and positive. Thus, if $V < 1$, the point $D_{\Omega=0}$ is located on the negative semi-axis and the clamped-pinned pipe is stable.

Table 1: Parameters used in the calculations

Parameter				Dimensionless Parameter	
EI	$1.00{*}10^9$ Nm^2	T_{eff}	$1.00{*}10^6$ N	α	2.24
m_f	$1.00{*}10^3$ kg / m	L	100 m	β	10.0
m	$2.00{*}10^3$ kg / m	C_d	1.00 m/s	γ	3.54
D	1.00 m	ρ_f	$1.00{*}10^3$ kg / m^3		

6 Damped clamped-pinned system

In this section, it is demonstrated that the D-decomposition method is a convenient tool for the stability analysis of pipes with distributed losses. To show this, a pipe subject to linearised Morison damping is considered, as shown in Figure 2. As compared to the undamped case, the Morison drag modifies the relationship between the eigenvalues λ and wavenumbers k_j to the following form

$$k_j^{\,4} - \beta\left(V^2 - 1\right)k_j^{\,2} + 2\alpha V \lambda i k_j + \lambda^2 + \gamma\lambda = 0 \tag{33}$$

The characteristic equation Eq.(18) and the mapping rule Eq.(19), however, remain the same, with A and B defined in Appendix A. In the presence of finite damping, there is no need to evaluate the mapping rule analytically, since no significant numerical errors occur in this case.

To study the stability of the pipe, the system parameters shown in Table 1 are used. The result of D-decomposition of the $\kappa-$ plane is shown in Figures 6 and 7 for two fluid speeds: $V = 0.32$ (sub-critical) and $V = 2.05$ (super-critical), respectively. Only the key (low-frequency) part of the D-decomposition curves has been plotted in the figures. Taking higher frequencies into account would lead to more quasi-circles both in the lower and upper half planes. These circles, however, do not cross the real axis and therefore are of no significance for the stability analysis.

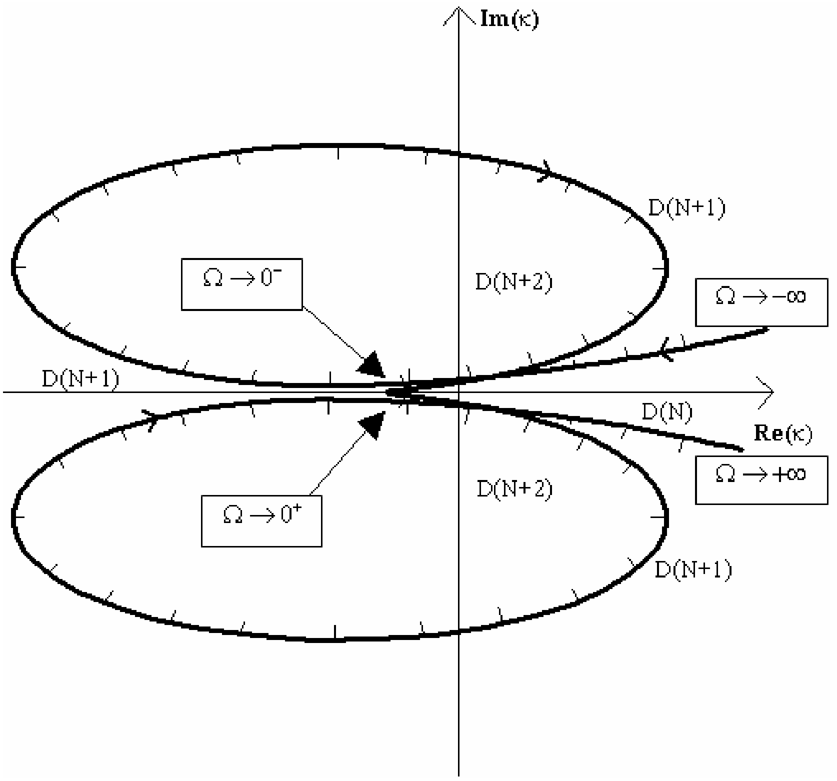

Figure 6: D-decomposition of the κ-plane for $V = 0.32$ (pipe subject to Morison damping).

Figure 6 shows that in the sub-critical case, $V = 0.32$, the result of the D-decomposition is similar to that presented in Figure 5 for the pipe without damping. In both figures, the D-decomposition curves do not cross the positive part of the real axis. This means that the pipe's stability at this velocity does not depend on the stiffness of the rotational spring. Utilising again the known fact that the clamped-clamped pipe is stable at any fluid speed with or without the damping, we conclude that the clamped-pinned pipe is also stable if the flow speed is sub-critical.

The main difference between Figure 7 and Figures 5 and 6 is that in the former figure the D-decomposition curves cross the positive part of the real axis. Taking into account the direction of the shading, this implies that there is a critical stiffness of the rotational spring (the co-ordinate of the crossing point) below which the pipe is for sure unstable. Thus, if the flow is super-critical ($V = 2.05$), the clamped-pinned pipe is unstable. The critical velocity corresponds to the situation, when the D-decomposition curves cross the origin of the $\kappa-$ plane.

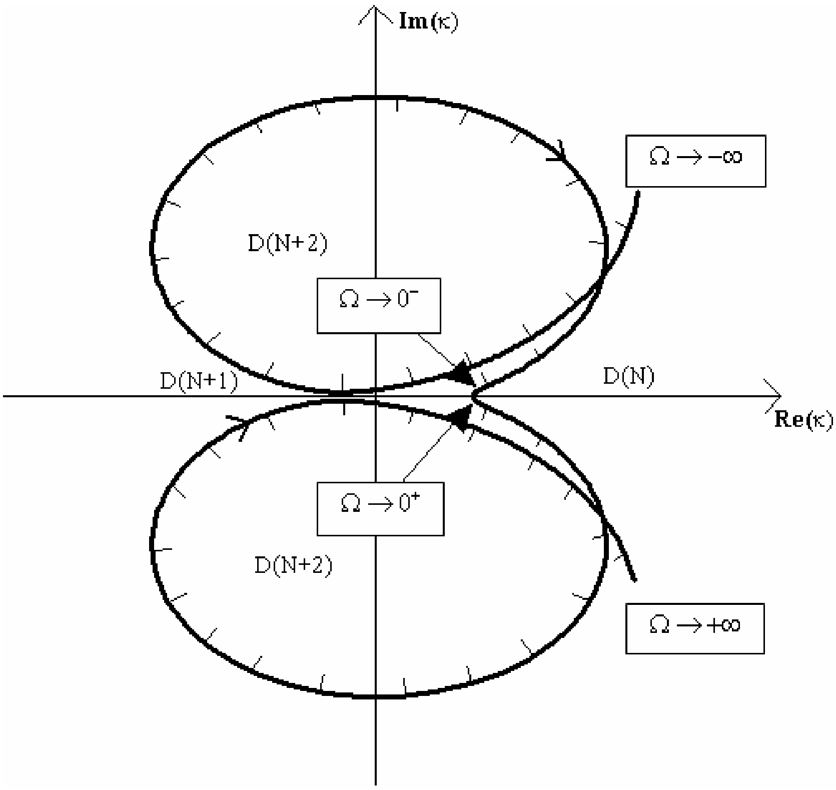

Figure 7: D-decomposition of the κ-plane for $V = 2.05$ *(pipe subject to Morison damping).*

The critical velocity can be found analytically since the crossing point $D_{\Omega=0}$ between the D-decomposition curves and the real axis corresponds to $\Omega = 0$. The coordinate of this point is given by the limit $\Omega \to 0$ of the ratio $-B/A$:

$$D_{\Omega=0} = \lim_{\Omega\to 0} \kappa = \frac{\zeta^2\left(1 + i\zeta - e^{2i\zeta} + i\zeta e^{2i\zeta}\right)}{4i\zeta e^{i\zeta} - \zeta^2 e^{2i\zeta} + \zeta^2 - 2i\zeta - 2i\zeta e^{2i\zeta}}, \qquad \zeta = \sqrt{\beta\left(V^2 - 1\right)}, \tag{34}$$

Studying Eq.(34), it can be shown that increasing V from 1, the point $D_{\Omega=0}$ moves along the real axis of the $\kappa-$ plane from the left half-plane to the right half-plane, crossing the origin as soon as the following equation is satisfied:

$$\tan(\zeta)-\zeta=0 \tag{35}$$

The first non-trivial solution of Eq.(35), $\zeta=\zeta_1$, is approximately given as $\zeta_1=4.4934$. Thus, if the velocity of the fluid is larger than the following critical velocity

$$V_{crit}=\sqrt{\frac{(\zeta_1)^2}{\beta}+1} \tag{36}$$

the clamped-pinned pipe becomes unstable. Using original parameters of the system, the expression for the critical velocity can be rewritten as

$$U_{crit}=\sqrt{\frac{(\zeta_1)^2 EI}{m_f L^2}+\frac{T_{eff}}{m_f}} \tag{37}$$

From this expression one can see that the linearised Morison damping does not influence the critical velocity. This can be expected for a system which loses stability by divergence. Note that the critical velocity is also independent of the mass of the pipe.

Since we proved here that the clamped-pinned pipe loses stability by divergence, the critical velocity can be computed much easier with the help of the static problem statement:

$$\frac{\partial^4\eta}{\partial\xi^4}+\beta\left(V^2-1\right)\frac{\partial^2\eta}{\partial\xi^2}=0$$

$$\eta(0)=0\,,\quad \frac{\partial\eta(0)}{\partial\xi}=0\,,\quad \frac{\partial^2\eta(1)}{\partial\xi^2}=0\,,\quad \eta(1)=0\,, \tag{38}$$

Solving this problem, it is easy to find that the critical velocity is determined by Eq.(35).

7 Conclusions

The stability of a tensioned clamped-pinned pipe conveying fluid has been considered. It has been proven analytically that for small fluid velocities this pipe is stable. It has been shown that the pipe

loses stability by divergence at relatively high fluid velocities. The critical velocity has been found analytically and has shown to be independent of the external linearised Morison damping.
The study has been accomplished with the help of a D-decomposition method developed by Neimark (1978). Advantages and disadvantages of this method relative to the conventional methods have been discussed. From the point of view of the authors, this method can be conveniently used in combination with the conventional methods to perform parametric studies of stability of various pipes conveying fluid. The method can easily be applied to other types of fluid-structure-instability, like flutter. Generally speaking, the method is not limited to linear systems. The stability of equilibrium points and limit cycles in nonlinear systems can be determined by using the D-decomposition method as well.

References

Denisov, G. G., Kugusheva, E. K., Novikov, V. V., 1985. On the problem of the stability of one-dimensional unbounded elastic systems. Journal of Applied Mathematics and Mechanics 49, 533-537.

Fuchs, B.A., Shabat B.V., Berry, T.J., 1964. Functions of Complex variables and some of their applications. Pergamon, Oxford.

Ginzburg, V.L., 1990. Applications of electrodynamics in theoretical physics and astrophysics. Gordon and Breach, New York.

Ginzburg, V.L., Tsytovich, V.N., 1990. Transition radiation and transition scattering. Hilger, Bristol.

Korn, G.A., Korn, T.M., 1961. Mathematical Handbook for Scientists and Engineers. McGraw-Hill Book Company, New York.

Lee, S.-Y., Mote, C.D., 1997. A generalized treatment of the energetics of translating continua, part I: strings and tensioned pipes. Journal of Sound and Vibration 204, 717-734.

Lee, S.-Y., Mote, C.D., 1997. A generalized treatment of the energetics of translating continua, part II: beams and fluid conveying pipes. Journal of Sound and Vibration 204, 735-753.

Matania, B-A., Devinatz, A., 1987. The limiting absorption principle for partial differential operators. American Mathematical Society, Providence.

Metrikine, A.V., Popp, K., 1999. Instability of vibrations of an oscillator moving along a beam on an elastic half-space. European Journal of Mechanics A / Solids 18(2), 331-349.

Metrikine, A.V., Verichev, S.N., 2001. Instability of vibrations of a moving two-mass oscillator on a flexibly supported Timoshenko beam. Archive of Applied Mechanics 71, 613-624.

Misra, A.K., Wong, S.S.T., Païdoussis, M.P., 2001. Dynamics and stability of pinned-clamped and clamped-pinned cylindrical shells conveying fluid. Journal of Fluids and Structures 15, 1153-1166.

Neimark, Yu.I., 1978. Dynamic Systems and Controllable Processes. Nauka, Moscow (in Russian).

Neimark, Yu.I., Golumov, V.I., Kogan M.M., 2003. Mathematical models in natural science and engineering. Springer, Berlin.

Païdoussis, M.P., Tian, B., Misra, A.K., 1993. The dynamic and stability of pinned-clamped coaxial cylindrical shells conveying viscous flow. Proceedings of the Canadian Congress of Applied Mechanics, CANCAM 93, Queen's University, Kingston, Ontario, 259-260.

Païdoussis, M.P., 1998. Fluid-Structure Interactions: Slender Structures and Axial Flow, Vol. 1. Academic Press, London.

Païdoussis, M.P., 2004. Fluid-Structure Interactions, Vol. 2. Academic Press, London.

Verichev, S.N., Metrikine, A.V., 2002. Instability of a moving bogie on a flexibly supported Timoshenko beam. Journal of Sound and Vibration 253(3), 653-668.

Zheng, D. Y., Au, F. T. K., Cheung, Y.K., 2000. Vibration of vehicle on compressed rail on viscoelastic foundation. ASCE, Journal of Engineering Mechanics 126(11), 1141-1147.

Zolotarev, I., 1987. Optimization of aerodynamic damping of a cylindrical shell with flowing fluid with the aid of boundary conditions. Mashinovedenie 1, 49-55.

Appendix A: The characteristic equation

The determinant of the system Eq.(17) reads

$$\Delta = \kappa \cdot A + B, \tag{1}$$

$$A = -\Big\{ k_2k_3e^{i(k_3+k_4)} + k_1k_3e^{i(k_2+k_3)} - k_3k_4e^{i(k_2+k_3)} - k_1k_2e^{i(k_1+k_4)} + k_3k_4e^{i(k_1+k_3)}$$

$$-k_2k_4e^{i(k_3+k_4)} - k_2k_3e^{i(k_1+k_3)} - k_1k_2e^{i(k_2+k_3)} - k_1k_4e^{i(k_2+k_4)} + k_2k_3e^{i(k_2+k_3)}$$

$$+k_1k_2e^{i(k_2+k_4)} - k_3k_4e^{i(k_1+k_4)} - k_1k_3e^{i(k_1+k_2)} - k_1k_4e^{i(k_1+k_3)} - k_1k_3e^{i(k_3+k_4)}$$

$$+k_2k_4e^{i(k_2+k_3)} + k_2k_4e^{i(k_1+k_4)} + k_2k_3e^{i(k_1+k_2)} - k_2k_4e^{i(k_1+k_2)} + k_1k_4e^{i(k_1+k_2)}$$

$$+k_1k_4e^{i(k_3+k_4)} + k_1k_3e^{i(k_1+k_4)} + k_3k_4e^{i(k_2+k_4)} + k_1k_2e^{i(k_1+k_3)} \Big\}$$

$$B = i\Big\{ k_2{}^2k_3\,e^{i(k_2+k_4)} + k_2k_3{}^2e^{i(k_1+k_3)} + k_3{}^2k_4e^{i(k_2+k_3)} + k_1k_4{}^2e^{i(k_2+k_4)} - k_2k_3{}^2e^{i(k_3+k_4)}$$

$$-k_3k_4{}^2e^{i(k_2+k_4)} - k_2{}^2k_3e^{i(k_1+k_2)} - k_2{}^2k_4e^{i(k_2+k_3)} - k_1k_3{}^2e^{i(k_2+k_3)} - k_1k_2{}^2e^{i(k_2+k_4)}$$

$$-k_3{}^2k_4e^{i(k_1+k_3)} - k_2k_4{}^2e^{i(k_1+k_4)} - k_1k_4{}^2e^{i(k_3+k_4)} + k_3k_4{}^2e^{i(k_1+k_4)} + k_2{}^2k_4e^{i(k_1+k_2)}$$

$$+k_1 k_3^2 e^{i(k_3+k_4)} - k_1^2 k_4 e^{i(k_1+k_2)} + k_1^2 k_4 e^{i(k_1+k_3)} + k_1^2 k_2 e^{i(k_1+k_4)} - k_1^2 k_2 e^{i(k_1+k_3)}$$

$$\left. -k_1^2 k_3 e^{i(k_1+k_4)} + k_2 k_4^2 e^{i(k_3+k_4)} + k_1^2 k_3 e^{i(k_1+k_2)} + k_1 k_2^2 e^{i(k_2+k_3)} \right\}$$